Energy and size fluctuations of amphiphilic aggregates in a lattice model

Aniket Bhattacharya† and S D Mahanti

Department of Physics and Astronomy, Michigan State University, East Lansing, MI 48824-1116, USA

E-mail: `aniket@pa.msu.edu`

Abstract. We have studied the self-assembly of amphiphiles over wide ranges of temperature and concentration using Monte Carlo simulation of a lattice model introduced by Care. A new feature that we have observed is that for all the concentrations studied, the specific heat exhibits a peak as a function of temperature. The physical origin of this peak can be traced back to energy fluctuations occurring at the onset of micelle formations and can be used to characterize the critical micelle concentration (CMC). Our observations (i) that the temperature dependence of the specific heat fits rather well with the Schottky-type specific heat of a degenerate two-level system and (ii) that there is the simultaneous appearance of a knee in the cluster distribution function (CDF) explain the underlying physics of identifying the CMC with the appearance of this knee in the CDF, as proposed by Nagarajan and Ruckenstein. We show that the various moments of the cluster distribution functions can be expressed solely in terms of the second moment as predicted by a mean-field theory of Blankschtein, Thurston, and Benedek. We also calculate the fluctuation in the amphiphilic aggregate sizes and relate our simulation results to those from a simple but exactly soluble model proposed by Israelachvili.

(Some figures in this article are in colour only in the electronic version; see `www.iop.org`)

1. Introduction

An amphiphilic molecule consists of a hydrophobic tail, often a hydrocarbon chain, and a hydrophilic head. Because of the presence of these two opposing interactions towards the solvent in which they are immersed, amphiphiles can form a variety of structures, e.g., spherical and cylindrical aggregates (called micelles), bilayers, and vesicles [1]. Surfactants which are used in making soap and in the petrochemical industries, di-block and tri-block co-polymers, and phospholipids which form the cell membrane are a few examples of amphiphiles [2]. Understanding the physics of self-association of amphiphiles is extremely challenging and also important because the underlying ideas have found connections to other fundamental areas, e.g. phase transitions in membranes, crumpled surfaces, and geometry of random surfaces [4]. Furthermore, syntheses of novel nano- and meso-structured materials have been achieved by a surfactant-directed templating route, to produce ordered hexagonal arrays of cylindrical structures [5], disordered worm-like structures [6], and sponge-like porous structures [7]. Synthesis of a wide variety of structures using short di-block and tri-block co-polymers has

also gained considerable attention in designing and fabricating intricate patterns spanning many length scales [8].

Analytical theories disregarding the detailed shapes of the amphiphiles and incorporating ideas of geometric packing [2, 3], or a mean-field type of approach [9–16], have been able to predict several aspects of the aggregation process. Anything beyond a mean-field type of approach becomes immediately very difficult. Naturally, numerical simulations [17–35] have been extremely useful in addressing some of the fundamental and practical aspects of self-assembly. In order to get a thorough understanding of micellar aggregation as a function of temperature, concentration, and other external parameters, various coarse-grained models have been proposed which neglect the detailed chemical attributes of the amphiphiles. As a result, it is computationally feasible to study the aggregation properties of a large number of amphiphiles. Alternatively, numerical simulations respecting the geometrical and chemical attributes of the amphiphiles have also been attempted, but either at the cost of assuming a pre-assembled micellar structure, or restricting the study to a few micelles only [36]. Coarse-grained models whose basic ingredient is an unfavourable interaction between the hydrocarbon tails and the solvent water molecule have been able to predict micellar aggregation. More recent simulations eliminating the solvent degrees of freedoms have also been able to reproduce the aggregation properties of the amphiphiles [30, 31, 34, 35]. Typically, for continuum models, shifted Lennard-Jones interactions are assumed among different components of the amphiphiles with appropriate cut-off parameters for simulation of neutral systems. An extreme version of these coarse-grained models is the lattice model where amphiphiles are allowed to move on a lattice only. The lattice models have also been studied and have produced very similar results [18–24]. Simulation studies on lattice models have the additional advantage that the algorithms are very fast and fairly large systems can be studied.

In this paper we report several new results on thermodynamic and structural properties of the aggregation process based on Monte Carlo simulation on a lattice model introduced by Care and co-workers [18–21]. First we make a detailed comparison of analytic predictions of mean-field theories regarding characteristic features near the critical micelle concentration with our simulation results. Second, we show that a peak in the specific heat as a function of temperature is a general feature and identify the temperature as a characteristic temperature for micelle formations. Third, we test the recurrence relations among moments of the cluster distribution function derived from some general assumptions with our simulation results [10]. Finally we investigate the scaling of micellar size fluctuation as a function of concentration and compare this with the analytic result for an exactly solvable one-dimensional system. In the next section we introduce the model and describe the Monte Carlo simulation scheme.

2. Model

We have used a model introduced by Care [18–21] where the amphiphiles are confined to a two-dimensional square lattice of size $L \times L$. In this model each amphiphile is represented as a connected segment of s adjacent sites (chain length $= s$). One of the two end sites is the hydrophilic head, and the remaining $s - 1$ sites make the tail of the amphiphiles. Each amphiphile will also be called a monomer. We consider N_A of such amphiphiles which occupy sN_A lattice sites. The remaining $N_w = L \times L - sN_A$ sites are occupied by the solvent molecules. The total energy of the system is given by

$$H = \epsilon_{TS} n_{TS} + \epsilon_{HS} n_{HS} + \epsilon_{HH} n_{HH} + \sum_i \epsilon_c^i \tag{1}$$

where n_{TS}, n_{HS}, n_{HS} are the total number of tail–solvent (TS), head–solvent (HS), and head–head (HH) bonds of strengths ϵ_{TS}, ϵ_{HS}, ϵ_{HH} respectively, and $\sum_i \epsilon_c^i$ represents the

conformation energy which may include bending energies as well. Defining $\gamma = \epsilon_{HS}/\epsilon_{TS}$ (ϵ_{TS} will be assumed to be always positive, indicating a repulsive interaction between a tail particle of the amphiphile and the solvent), $\eta = \epsilon_{HH}/\epsilon_{TS}$, $\bar{\epsilon}_i = \epsilon_i/\epsilon_{TS}$, the above equation can be written as

$$H = \epsilon_{TS}[n_{TS} + \gamma n_{HS} + \eta n_{HH}] + \sum_i \bar{\epsilon}_c^i. \tag{2}$$

The quantity γ is the most crucial parameter in this model. Care and co-workers have studied various aspects of this model in detail [18–21]. For $\gamma > 0$ there is a complete phase separation of the amphiphiles at low temperature, whereas for a negative value of γ there is a gain in energy caused by shielding the tail particles from the solvent, and one gets micelles of different shapes and sizes depending upon the chain length and particular choice of γ. Vesicles and bilayers have been observed in the numerical simulation of these types of lattice model [20,24]. For γ very small but negative, one gets large micelles. With larger negative values of γ, the average cluster size decreases.

We have carried out numerical simulations for a wide range of temperature and amphiphile concentration for several choices of γ. For simplicity, we have chosen $\eta = 0$, and $\epsilon_c^i = 0$. Most of our simulations are done in a 128×128 square lattice. Most of the results presented in this paper are for chain length $s = 3$ with one head and two tail particles. However, for comparison we have also studied larger chain lengths ($s = 6$). In a few cases we have also looked at larger lattice sizes to check the finite-size effects. Starting from a high-temperature phase at $T = 1.6$ (where the temperature is measured in units of ϵ_{TS}/k_B), we have reduced the temperature in steps of 0.02 and 0.01 to the lowest temperature of 0.42. For each temperature we have calculated the total energy, the specific heat, and the cluster (or aggregate) size distributions and their moments.

Monte Carlo moves consist of slithering snake reptation of the individual chains [37], kink jumps of the middle units, and rotation of the end units [38]. For high temperature the typical length of MC steps is $\sim 10^5$. For lower temperatures 10^7–10^8 MC steps were necessary for proper equilibration. To find out the concentration dependence of different physical quantities, we studied systems consisting of 32 to 1600 amphiphiles. For each concentration ensemble, averages were taken for 3–5 different initial configurations. Most of our results reported in this paper are for $\gamma = -0.6$.

3. Results

3.1. Critical micelle concentration

A ubiquitous feature of amphiphiles is the behaviour of unattached amphiphiles as a function of the total concentration. Let us denote by X_n the concentration of amphiphiles contained in aggregates of size n. Thus X_1 is the concentration of monomers, X_2 is the concentration of amphiphiles in dimers, etc. At very low concentrations, entropy favours them not to form micelles. As the concentration is increased, micelles of all sizes begin to form and this manifests itself as a rapid flattening of X_1 as a function of the total concentration X. In figure 1(a) we show the variation of X_1 as a function of X for different temperatures. It is customary to pick a value of X on the X_1-versus-X curve as the critical micelle concentration (CMC) X_{cmc}, beyond which X_1 hardly increases. There have been numerous efforts to characterize X_{cmc}. Ruckenstein and Nagarajan tried to equate X_{cmc} to that particular value of X (X_{RN}) whose corresponding cluster distribution exhibits a point of inflection [13, 14]. As X is increased beyond X_{RN}, the point of inflection becomes flat and eventually exhibits a minimum and a maximum as a function of the cluster size. Ben-Naim and Stillinger [15] (BS) studied a simple
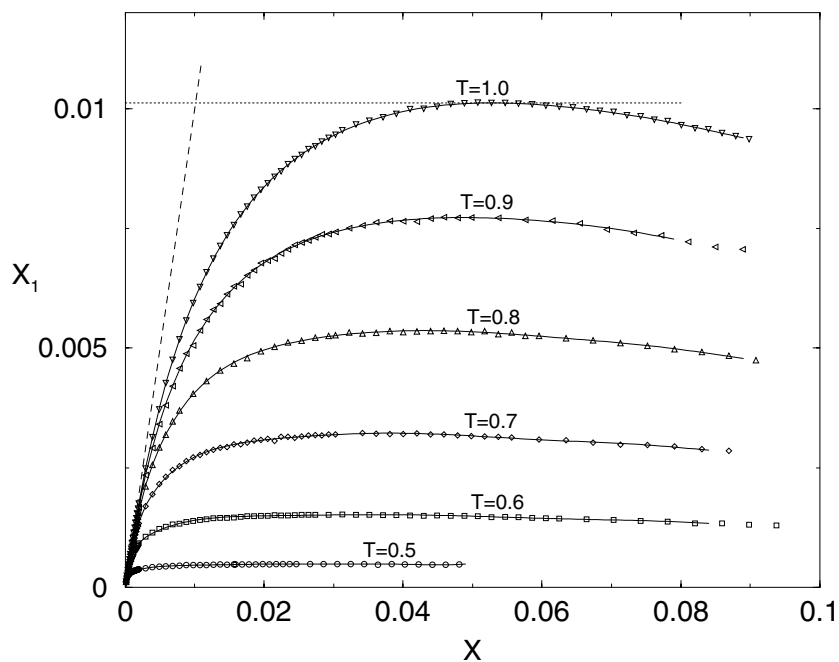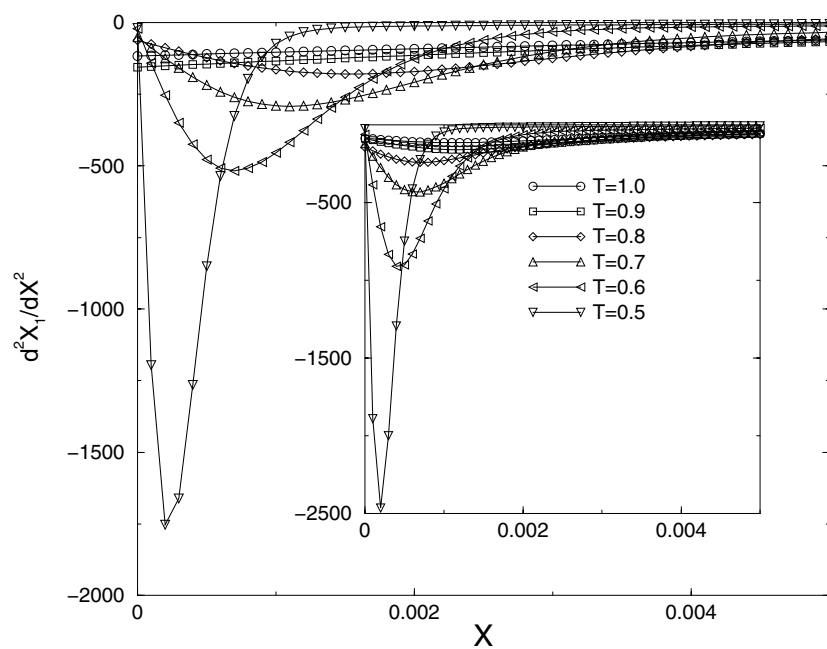
Figure 1. (a) The concentration of monomers X_1 as a function of the total concentration X of the amphiphiles for different temperatures. The symbols represent the data obtained from simulation and the straight lines are the corresponding polynomials fitted to the data. (b) Variation of $d^2 X_1/dX^2$ as a function of the total concentration X of the amphiphiles for different temperatures.

model of micellization and found that the X_{cmc} is better identified as that value of X (X_{BS}) for which the absolute value of $\mathrm{d}^2 X_1/\mathrm{d}X^2$ is a maximum, lending support to an idea originally proposed by Phillips [39]. In the BS model $X_{RN}/X_{BS} \approx 20$ and therefore Ben-Naim and Stillinger claimed that the Ruckenstein–Nagarajan criterion was not universal. It is worth pointing out that an undesirable feature of the BS model is that the above minimum in the cluster distributions instead of being smooth exhibits a cusp, probably resulting as an artifact of a sharp cut-off used in their model. Ruckenstein and Nagarajan made the criticism that the model used by Ben-Naim and Stillinger was unphysical and therefore did not disprove the assertion that one could associate X_{cmc} with the onset of a knee in the cluster distribution function.

We have fitted the curves in figure 1(a) with a polynomial:

$$f(x) = a_0 \tanh\left(\frac{x}{a_1}\right) + \sum_{n=2}^{n=8} a_n x^{n-1}.$$

Near $X \sim 0$ the slope

$$\lim_{x \to 0} \mathrm{d}X_1/\mathrm{d}X = 1.$$

The slope gradually decreases to zero and for large concentration becomes marginally negative. Care and co-workers [21] in their simulation observed this slight but noticeable negative slope. We have calculated $\mathrm{d}^2 f(x)/\mathrm{d}x^2$ and find that the maximum of $|\mathrm{d}^2 f(x)/\mathrm{d}x^2|$ occurs around $X = 0$ as shown in figure 1(b). The inset shows $\mathrm{d}^2 g(x)/\mathrm{d}x^2$, where the function $g(x)$ is similar to $f(x)$ except that the coefficient of the linear term is forced to be unity ($a_2 = 1 - a_0/a_1$) and fits the numerical data of figure 1(a) well. As the temperature decreases the minimum becomes sharper and shifts towards lower values of X. A comparison with figure 1(a) shows that the values of X at which the minima occur are indeed very close to $X = 0$. From our simulation results we have also looked at the cluster distributions as a function of X for various temperatures and located the approximate value of X where the cluster distribution shows a point of inflection. We find that, as the temperature increases, X_{RN} shifts to a larger value of X and *may occur in the flat region of figure 1(a), far away from the knee*. This is in qualitative agreement with the idea of Stillinger *et al* that the point of inflection need not necessarily be associated with the knee of figure 1(a). However, as we will see later, the RN criterion of associating the knee of the cluster distribution is physically very appealing and can be related to other indicators of self-association. The fact that we get a maximum of $\mathrm{d}^2 f(x)/\mathrm{d}x^2$ close to $X = 0$ is partly due to short amphiphiles and partly due to the two-dimensional simulation, both of which make the X_1-versus-X plot smoother. This is consistent with the analytic treatment of Stillinger and Ben-Naim [16] who, using the approach of Lee and Yang [40], concluded that no phase transition can be associated with X_{cmc} for finite-size micelles.

In order to carry out further analyses of our simulations results, we have adopted a working definition of X_{cmc} as the intercept of the horizontal line passing through a point where $\mathrm{d}X_1/\mathrm{d}X = 0$ and the line $X_1 = X$, as shown by the dotted line in figure 1(a). For larger and larger surfactants, keeping the head-to-tail ratio fixed, it is expected that the X_1-versus-X plot will approach the shape of the dotted curve. We denote this intercept as X_{cmc}^-. An alternative way to characterize X_{cmc} is to choose that particular value of X where $\mathrm{d}X_1/\mathrm{d}X = 0$. This is consistent with the idea that beyond this value of X (we call this X_{cmc}^+) X_1 either stays constant or decreases slightly. Both of these plots are shown in figure 2. An important and noticeable feature of figure 2 is a characteristic energy (temperature) ($T^* \approx 0.6$) beyond which X_{cmc}^- increases linearly and X_{cmc}^+ rises rapidly as a function of T. In the next section we will explain that this characteristic temperature T^* is an important quantity in understanding the physics
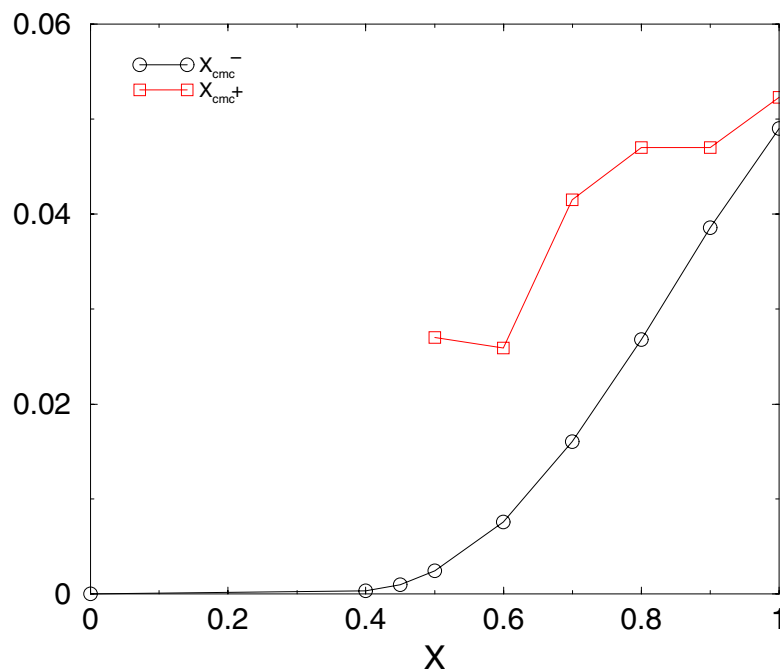
Figure 2. Variation of X_{cmc}^- and X_{cmc}^+ as a function of temperature. For comparison, X_{cmc}^- has been scaled by the factor 5.

of micellization and can be related to the knee of the cluster distribution function and other measurable quantities.

3.2. The peak in the specific heat and dX_1/dT

In this section we show the temperature variation of the specific heat and various quantities related to the distribution of amphiphiles among aggregates of different sizes. The specific heat at each temperature is calculated by monitoring the energy fluctuations ($\langle E^2 \rangle - \langle E \rangle^2 = \langle (\Delta E)^2 \rangle = k_B T^2 C_v$). In order to study the temperature dependence, starting from a high temperature ($T = 2$), the specific heat is calculated for each temperature as the system is slowly cooled to a final lower temperature ($T = 0.45$). The specific heat calculation is repeated while the system is heated again. No hysteresis in energy nor shift in the position of the peak is found, guaranteeing thermodynamic equilibrium. While for temperature around $T = 1$ and above, runs with two different initial conditions with $\sim 10^6$ Monte Carlo steps give almost identical results, for the lower temperatures $\sim 10^8$ MC steps are used. Accordingly, the interval for taking averages is increased to eliminate correlations between two successive measurements. The average is taken for 4 or 5 such runs with different initial random configurations of the amphiphiles, which eliminates spurious effects.

When plotted as a function of temperature, both the specific heat and the quantity (dX_1/dT) exhibit peaks as shown in figure 3 and figure 4. We have shown results for four different concentrations. We have checked that the occurrence of these peaks is a general feature. Let us now have a closer look at these figures. For each concentration the peak for dX_1/dT appears at a slightly higher temperature than the corresponding peak in the specific heat. The positions of both the peaks are weakly dependent on the total concentration X. Our simulation
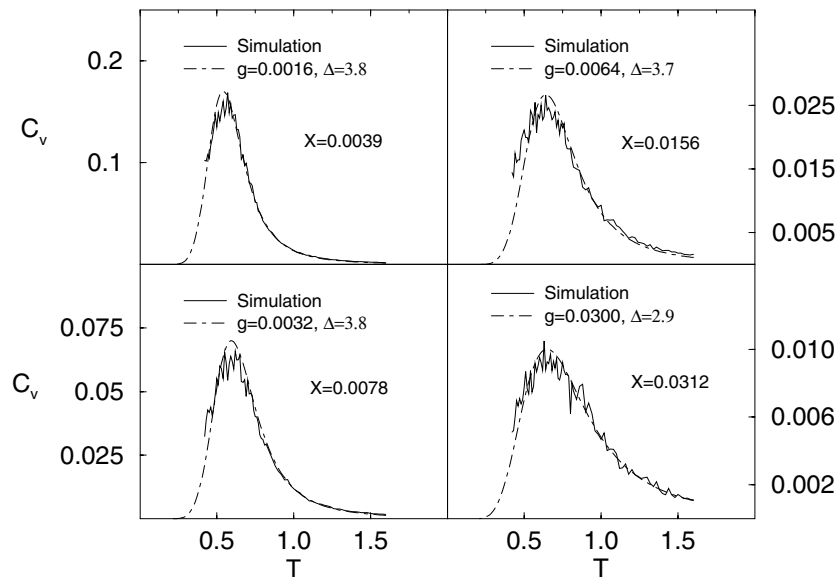
Figure 3. Specific heat as a function of temperature for four different concentrations of amphiphiles (solid line). The dot–dashed line is a fit using the expression for a Schottky-type specific heat for a degenerate two-level system with various values of the degeneracy ratio g (see the text) and Δ.
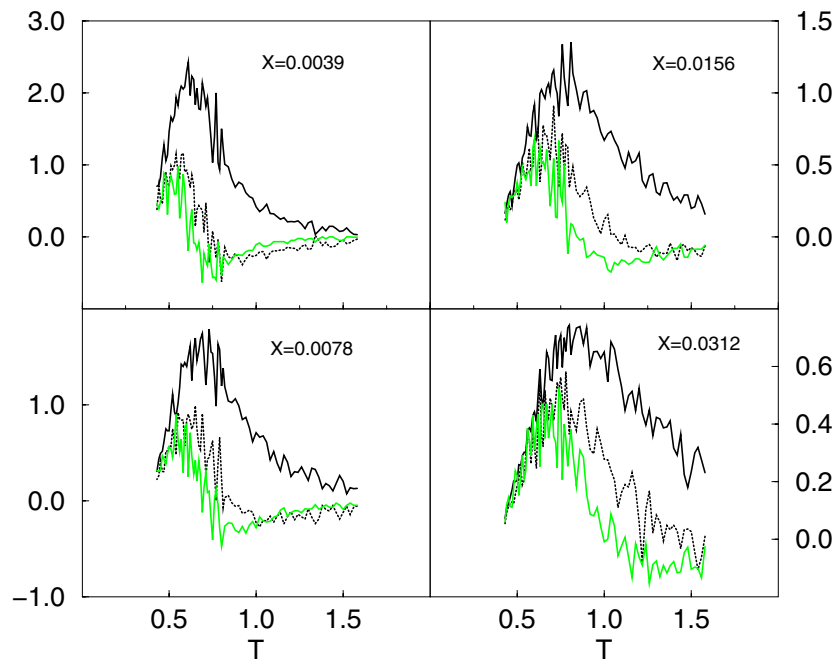

Figure 4. Variation of dX_1/dT (solid line), dX_2/dT (dashed line), and dX_3/dT (grey solid line) as a function of temperature for the same four different concentrations of amphiphiles as in figure 2.

data indicate that the peaks shift slightly to lower temperature with decreasing concentration. The specific heat data can be fitted reasonably well with a Schottky-type specific heat for a

degenerate two-level system [41] as indicated by the dashed lines in figure 3.

The weak concentration dependence of the position of the specific heat peak and the Schottky-type behaviour indicate that this phenomenon can be ascribed to the thermodynamics of a two-level system whose characteristic energy scale is also weakly concentration dependent. Besides, we also find that the peak for the specific heat and dX_1/dT are inter-related as explained below. Let us remind ourselves that for a two-level system separated by an energy gap Δ, the energy per particle is given by

$$E_{Schottky} = -\frac{\Delta}{2} \tanh\left[\frac{\Delta}{2kT} + \frac{1}{2}\ln(g)\right]$$

and the specific heat is given by

$$C_{Schottky} = \left[\frac{\Delta}{kT}\right]^2 \operatorname{sech}^2\left[\frac{\Delta}{2kT} + \frac{1}{2}\ln(g)\right] = \left(\frac{\Delta}{kT}\right)^2 \frac{ge^{\Delta/kT}}{[1 + g\Delta/kT]^2}$$

where $g = g_l/g_u$ is the ratio of the degeneracies g_l and g_u of the lower and upper energy levels respectively. For $g = 1$, the specific heat shows a peak for $\Delta/kT \sim 0.4$. For larger values of g the position of the peak shifts towards a lower value of Δ/kT. Therefore, for a *fixed* Δ, an *increase* in g will *shift the peak to a higher value of the temperature* (notice that g^{-1} is the relative degeneracy of the upper level compared to the lower level).

For the amphiphiles on a lattice, one can think of the energy levels in the following way. For these systems it is reasonable to assume that the minimum-energy configuration of an n-mer (an aggregate containing n amphiphiles) is a strip where every other head is on one side as shown in figure 5. For such a configuration, the total energy $E_n = (-3\gamma+1)n+4$. Consider the energy of dissociation $E_{gap} = E_n - (E_{n-m} + E_m)$, where an initial aggregate of size n breaks into two smaller aggregates of sizes m and $n-m$ respectively. For the one-dimensional geometry shown in figure 5, this energy difference $E_{gap} = 4$ for any $n \geqslant 2$ and $m \geqslant 1$.
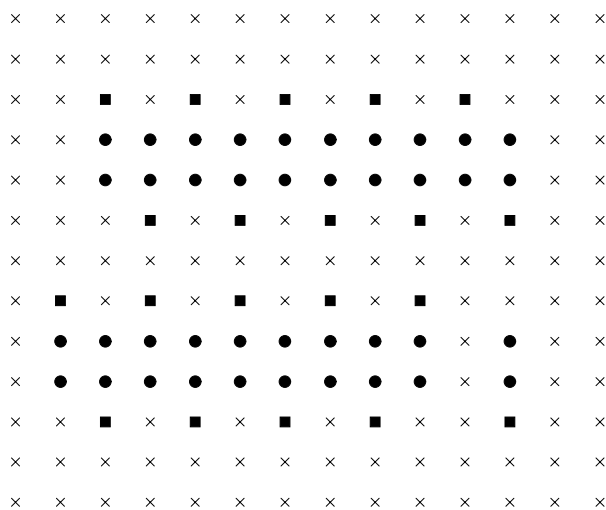

Figure 5. Excitation energy for one-dimensional micelles. The filled squares and circles represent the head and the tail of the amphiphiles, and the crosses are the solvent particles. The top part shows the minimum-energy configuration of a chain. The bottom part shows whether the configuration at the top breaks up into two fragments of sizes $n-1$ and 1. The energy difference in this case is $4\epsilon_{TS}$ caused by breaking two tail–tail bonds and exposing them to water. For this one-dimensional linear aggregate, the excess energy is the same as for an aggregate of size n breaking up into two clusters of sizes $n-m$ and m respectively for $n \geqslant 2$ and $m \geqslant 1$.

Table 1. Parameters for the degenerate Schottky model.

Lattice size	X	Δ	g
128×128	0.0039	3.8	0.0016
128×128	0.0078	3.8	0.0032
128×128	0.0156	3.7	0.0064
128×128	0.0312	2.9	0.0030

Table 1 gives the values of g and Δ for the fitted data shown in figure 3. For the first three concentrations, the data fit very well with a value of $\Delta \sim 4$ and a degeneracy factor which increases proportionally with the concentration. The slight shift in the peak temperature can thus be associated with the increase in the degeneracy factor. It is also worth noting that since $E_{gap} = 4$ is valid for all $n \geqslant 2$, and $m \geqslant 1$, this implies that for a given degeneracy factor g, associated with this $E_{gap} = 4$, there exists a temperature at which clusters of all sizes can break up into fragments of arbitrary smaller sizes giving rise to a large energy fluctuation. Our fit to the simulation data is consistent with the fact that with increasing concentration the available phase space decreases, which is reflected in a decrease (increase) in g^{-1} (g). As the concentration of the amphiphiles increases, further deviation from this simple theory becomes evident. For $X = 0.032$, the value of g varies significantly from linearity and the presence of the other amphiphiles makes the effective Δ less than 4. Nevertheless, it is worth noting that even in this case the energetics of the lattice amphiphiles can be described as an effective two-level system with a renormalized width and degeneracy parameter.

Now we give a physical picture of the Ruckenstein–Nagarajan criterion of identifying X_{cmc} with the knee of the cluster distribution. The peak in the specific heat implies the onset of rearrangement of amphiphiles which causes a large amount of energy fluctuation. As the temperature is lowered, clusters begin to form. This is also evident on looking at the cluster distribution function (CDF) X_n/n at different temperatures. At high temperature there is almost a monotonic decay of the CDF. At low temperature the CDF has a minimum followed by a maximum which then decays to zero for large n. For each concentration, we looked carefully at the CDF in the temperature region around which the specific heat peak occurs. We find that the CDF is marked with the onset of a knee [13] at the same temperature for which the peak occurs for the specific heat as shown in figure 6(c). Below this temperature, the knee becomes flat for several values of n and eventually exhibits a maximum at a lower temperature. Alternatively, for the same temperature we have checked that the cluster distributions exhibit similar features as a function of the total concentration. Our interpretation of the heat capacity in terms of a Schottky type of behaviour is also consistent with this observation. The flattening of the CDF actually means that clusters of different sizes begin to appear. This occurs at the temperature corresponding to the Schottky gap when it becomes energetically favourable for two amphiphiles to bind together. We can now also explain the observed peak in dX_1/dT. Assuming a negligible inter-micelle interaction (because of the short-range nature of inter-amphiphile interaction), the total energy of the system can be written as

$$E = \epsilon_1 X_1 + \epsilon_2 X_2 + \epsilon_3 X_3 + \cdots. \tag{3}$$

The heat capacity will have two contributions, one from the temperature dependence of X_i and the other from the temperature dependence of the energy ϵ_i of each micelle of size i. At temperatures of interest we expect the latter to be rather small and we can write the heat capacity as

$$C_v = \frac{dE}{dT} = \epsilon_1 \frac{dX_1}{dT} + \epsilon_2 \frac{dX_2}{dT} + \epsilon_3 \frac{dX_3}{dT} + \cdots. \tag{4}$$
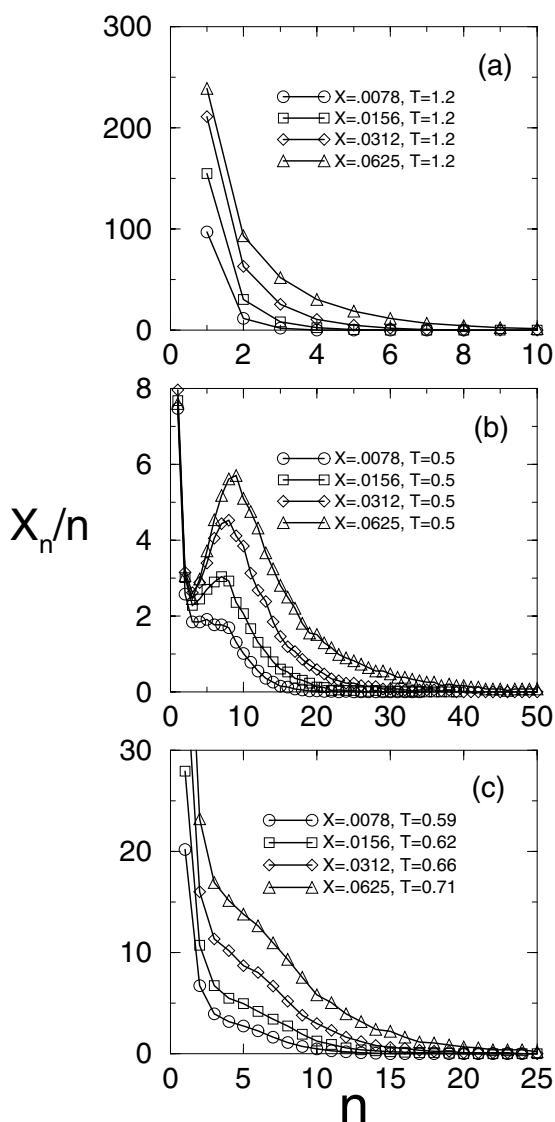
Figure 6. Variation of X_n/n for different X; (a) at $T = 1.2$, (b) at $T = 0.50$ for $X = 0.0078$ ($\circ$), 0.0156 ($\square$), 0.03125 ($\diamond$), and 0.0625 ($\triangle$); (c) the onset of a knee at different temperatures $T = 0.59$ ($\circ$), 0.62 ($\square$), 0.66 ($\diamond$), and 0.71 ($\triangle$) for the same concentrations as in (a) and (b).

In figure 4 we have shown the plots for dX_2/dT and dX_3/dT. They also exhibit peaks but at successively lower temperatures compared to the peak of dX_1/dT. This results in a shift of the peak of dE/dT to a lower temperature and explains why the peak of dX_1/dT occurs at a higher temperature than the corresponding peak in dE/dT.

We have also looked at the distribution of the X_n for different concentrations and temperatures. For a given concentration, comparing the distribution functions for X_n and X_n/n as a function temperature we find that the knee for X_n occurs at a higher temperature. This is shown in figure 7. Figure 7(a) shows the appearance of knees at various concentrations. When compared with figure 6(c), the temperature for which the knees occur are higher than the corresponding temperatures shown in figure 6(c). For the same set of temperatures as in figure 6(c) the X_n have already developed peaks as shown in figure 7(b). The factor n in the denominator of X_n/n competes with the rise of X_n as a function of n. Hence a peak in X_n at
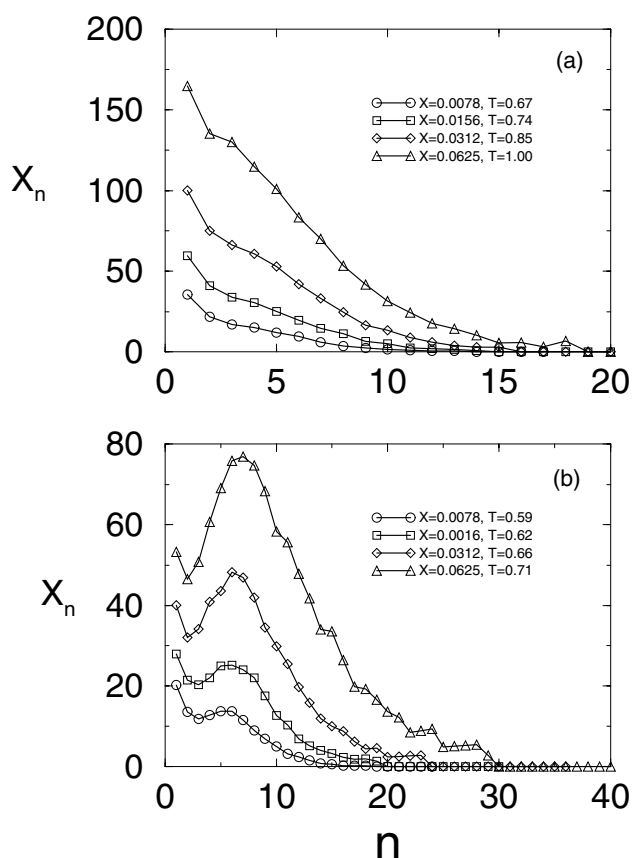
Figure 7. Appearance of a knee in X_n for the same set of concentrations as in figure 6(c). The temperatures at which they occur are $T = 0.67$ (○), 0.74 (□), 0.85(◇), and 1.00 (△) respectively; (b) shows X_ns for identical parameters to those of figure 6(c) for comparison.

a finite n shows up in X_n/n only when the peak in X_n becomes much more pronounced, such that the damping effect of n does not remove the peak in X_n/n. As a result one sees a finite-n peak in X_n/n at a lower temperature. We also checked that just as the appearance of a knee in the CDF can be associated with the peak in C_v, in a similar fashion, a knee appears for X_n at the temperature where dX_1/dT exhibits a peak.

One may wonder whether the arguments given above for small amphiphiles ($N_m = 3$) (with one head and two tail particles) are tenable for larger amphiphiles. We have verified that the analysis based on a two-level system is also valid for larger amphiphiles. For the sake of comparison we have carried out two other sets of simulations. We have repeated the simulation for the same amphiphiles but in a larger box keeping the density the same. The other simulation was carried out for (longer) amphiphiles ($N_m = 6$) with two head and four tail particles. The results for the T-dependence of C_v are shown in figure 8. The circles and the squares are for smaller ($N_m = 3$) amphiphiles for two different system sizes. The diamonds correspond to the $N_m = 6$ system. First, it is to be noticed that the finite-size effects are almost negligible when we compare the values for specific heat for the two $N_m = 3$ systems. Secondly, larger amphiphiles ($N_m = 6$) also have the same feature. We checked that for the same density of amphiphiles, peaks for the larger amphiphiles occur at a higher temperature, corresponding to
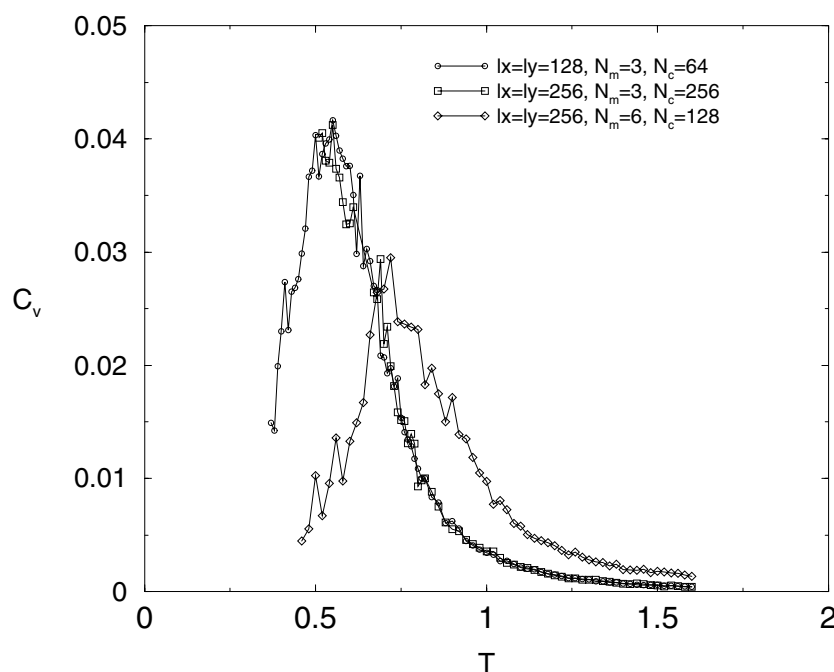
Figure 8. Comparison of specific heats for three different systems. The circles are for 64 amphiphiles each consisting of one head and two tail particles confined in a 128×128 simulation box. The squares are for the same type of amphiphile but for a larger system (256 amphiphiles confined in a 256×256 simulation box). The diamonds are for 128 amphiphiles confined in a 256×256 simulation box where each amphiphile consists of two head and four tail particles. Here the monomer density is the same but the chain concentration is half that of the previous system (squares). This shows that the peak is a generic feature and a characteristic of micelle formation.

a higher value of the energy of dissociation E_{gap}.

It is worth noting that the explanation in terms of a two-level system is also consistent with the temperature dependence of X^-_{cmc} and X^+_{cmc} shown in figure 2. The structure and size of the amphiphiles set an approximate energy scale. This energy scale comes out through various quantities. The temperature variation of X_{cmc} and the peaks in the temperature dependences of different physical quantities reflect that around a certain characteristic temperature, reorganization of the individual amphiphiles begins to occur.

Finally, the entropic contributions even for $N_m = 3$ amphiphiles are comparable with the binding energies. It is easy to check that the entropy for two amphiphiles [42] shown in figure 5 is $kT \ln(12)$, and the ground-state energy is $6(1 + \gamma)$. For $T = 0.6$ and $\gamma = -0.6$, the energy is 2.4 and the entropic contribution is 1.49, comparable to the binding energy. Therefore we believe that this simple model even with short amphiphiles exhibits the generic features of self-assembly.

3.3. Comparison with analytic theories

We now relate our simulation results to several existing theoretical predictions. Analytic theories of self-association of amphiphiles have traditionally relied on minimizing the total Gibbs free energy G which consists of three additive parts, G_f, G_m, and G_{int} [10]:

$$G = G_f + G_m + G_{int}. \tag{5}$$

G_f is given by

$$G_f = N_w \mu_w^0 + \sum_n N_n \mu_n^0 \tag{6}$$

where μ_w^0 and μ_n^0 are the intrinsic free energies of a solvent molecule and a micelle of size n respectively. N_w and N_n are the total number of solvent molecules and the number of micelles of size n respectively. The free energy of mixing often has the form

$$G_m = k_B T \left[N_w \ln(X_w) + \sum_n N_n \ln\left(\frac{X_n}{n}\right) \right] \tag{7}$$

where

$$X_w = \frac{N_w}{N_w + N_s} \qquad X_n = \frac{n N_n}{N_w + N_s}$$

and k_B is the Boltzmann constant. Here we have followed the notation of Israelachvili [2] and have used X_n to denote the total concentration of amphiphiles forming aggregates of size n. Therefore the concentration of aggregates of size n is X_n/n, and the total concentration $X = \sum_{n=1}^{\infty} X_n$. A Flory–Huggins type of free energy of mixing has also been used [11]. G_{int} describes the interaction among the micelles. In the treatment of Blankschtein and co-workers, G_{int} is approximated as

$$G_{int} = -\frac{1}{2} \sum_i N_i U_i \tag{8}$$

where $U_i = \sum_j f_{ij} \rho_j$ and ρ_j is the density of micelles of size j (j-mers). In the above equation the interaction energy has been introduced in a mean-field fashion so that an i-mer interacts with the average potential generated from other j-mers. Minimizing the free energy and invoking the idea of multiple chemical equilibria yields the well known result

$$X_n = n\{X_1 \exp[-\beta(\mu_n^0 - n\mu_1^0)]\}^n \exp\left[\beta \sum_j (f_{nj} - n f_{1j}) \rho_j\right]. \tag{9}$$

Blankschtein *et al* further assume infinite-range interaction among the micelles so that $f_{ij} = ij$. For this particular type of interaction, the second exponential term in equation (9) becomes unity and the result is exactly the same as if the inter-micelle interactions were absent. For this special form of interaction, the coexistence curve, spinodal line, etc, can be expressed solely in terms of the second moment of the micellar distribution (CDF), where the pth moment is defined as

$$M_p = \sum_n n^p \left[\frac{X_n}{n}\right]. \tag{10}$$

When the interaction term in equation (9) drops out, it is easy to check that

$$M_{p+1} = M_2 \left(\frac{\mathrm{d}M_p}{\mathrm{d}X}\right). \tag{11}$$

We have carried out simulations for a large number of concentrations so that the above results are amenable for further verification for the lattice amphiphiles. In order to check this recurrence relation we have calculated the second and the third moment of the cluster distribution (M_2 and M_3) which are shown in figure 9 for several different temperatures. The circles, squares, and diamonds are the data obtained from the simulation. The solid line in figure 9(a) is a polynomial fit
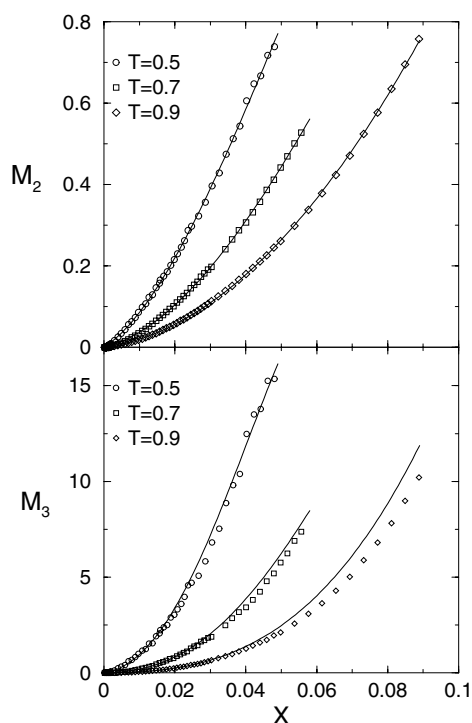
$$M_2^{poly} = \sum b_n X^n$$

Figure 9. Variation of M_2 (top) and M_3 (bottom) as functions of concentration for different temperatures. The circles, squares, and diamonds correspond to the simulation results for $T = 0.5$, 0.7, and 0.9 respectively. The solid lines in the top figure are polynomial fits to the data for M_2. The solid lines in the bottom figure correspond to $M_2(dM_2/dX)$ obtained from the numerical differentiation of M_2 (see the text).

to the simulation data. The solid line in figure 9(b) represents the calculated quantity $M_2^{poly} \, dM_2^{poly}/dX$. The agreement between this quantity and M_3 is extremely good below the characteristic temperature T^* mentioned earlier. At higher temperature the simulation results lie slightly below those calculated from equation (11).

3.4. Scaling of moments and comparison with simple models

We have analysed the distribution of amphiphiles of different sizes using the following quantity σ:

$$\sigma = \sqrt{\left(\sum_i i^2 n_i\right) \bigg/ \left(\sum_i n_i\right) - \bar{n}^2} \tag{12}$$

where the n_i are the numbers of clusters of size i and $\bar{n}$ is given by

$$\bar{n} = \left(\sum_{i=1}^{\infty} i n_i\right) \bigg/ \left(\sum_{i=1}^{\infty} n_i\right). \tag{13}$$

We can define the probability of occurrence of a cluster of size i as $p_i = n_i/\sum_i n_i$ so that $\sum_i p_i = 1$. Then it follows that the quantity $\bar{n} = \sum_i i p_i$ is the average cluster size and $\sigma = \sqrt{i^2 p_i - (i p_i)^2}$ is indeed a measure of the size fluctuation of clusters.

The quantity σ has been studied by Care and co-workers [19] and it is convenient to extract information regarding the polydispersity of the amphiphilic aggregation using σ. Analysing the instantaneous configurations of the cluster aggregation, we find that the simple amphiphiles (with one head and two tail particles) form elongated structures as shown in figure 10. This prompted us to look at the variation of σ in an exactly solvable model for one-dimensional rod-like micelles. Before we present our numerical results we briefly review some analytic
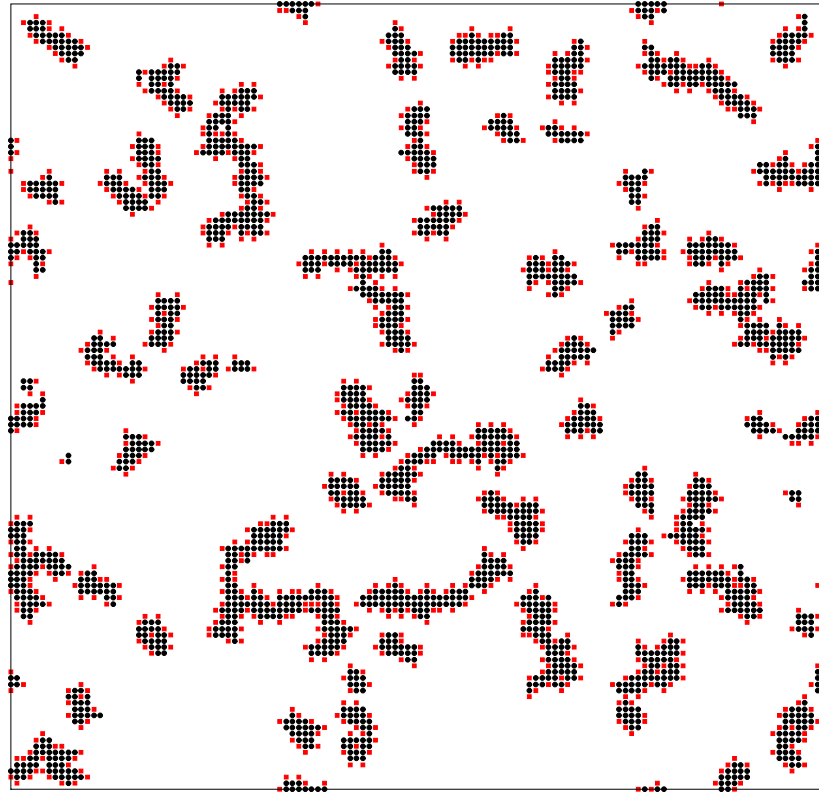
Figure 10. A snapshot of micelle formation at $T = 0.45$ for 1024 amphiphiles in a 128×128 box. The circles and the squares represent the tail and the head units respectively.

results for the one-dimensional micelles following Israelachvili [2]. In its simplest form the condition for the micelle formation is given by

$$\mu = \mu_1^0 + kT \ln(X_1) = \mu_2^0 + \frac{kT}{2} \ln \frac{X_2}{2} = \cdots = \mu_n^0 + \frac{kT}{n} \ln \frac{X_n}{n} \tag{14}$$

from which it follows that

$$X_n = n\{X_1 \exp[(\mu_1^0 - \mu_n^0)/kT]\}^n. \tag{15}$$

For elongated micelles of size n, if we assume that the average binding energy for any two amphiphiles is $\alpha k_B T$ (where α is a measure of the binding energy relative to the temperature), then the total energy for the aggregate of size n is $(n-1)\alpha k_B T$. The average chemical potential per amphiphile (neglecting the intra-micellar entropy contributions) is then given by

$$\mu_n^0 = \mu_\infty^0 + \frac{\alpha kT}{n}. \tag{16}$$

For this particular n-dependence of μ_n^0, X_n takes the following simple form:

$$X_n = n[X_1 e^\alpha]^n e^{-\alpha} \tag{17}$$

and the X_n satisfy the sum rule

$$\sum_{i=1}^{\infty} X_i = X \tag{18}$$

where X is the total concentration of the amphiphiles. For the case where the X_i have the simple form as expressed in equation (17), the above sum is just a geometric one and, therefore, everything can be analytically expressed in terms of the total concentration X and the parameter α (see the appendix). For example, p_i can be written as

$$p_i = (X_1 e^\alpha)^{i-1}[1 - X_1 e^\alpha] \tag{19}$$

where X_1 is given by

$$X_1 = \frac{(1 + 2Xe^\alpha) - \sqrt{(1 + 4Xe^\alpha)}}{2Xe^\alpha}. \tag{20}$$

It also follows that $\sigma = \sqrt{Xe^\alpha}$. In this rather simple model, for different concentrations of the amphiphiles X, the quantity $\sigma/\sqrt{X}$ becomes a function of α only, shown as the left inset of figure 11. For high temperature (i.e., for small α), $\sigma/\sqrt{X} \to 1$, and for low temperature it diverges as shown in figure 11. It is worth pointing out in this context that this divergence of σ at low temperature is a signature of the fact that the distributions of the p_i tend to be more uniform as the temperature decreases as shown in the right inset of figure 11.
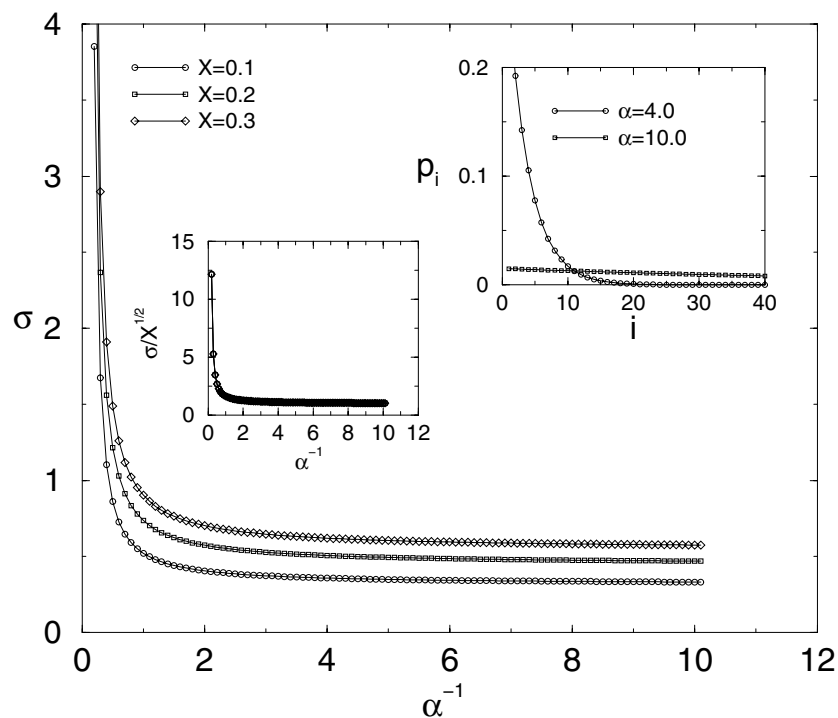

Figure 11. The variation of σ as a function of α^{-1} for $X = 0.1$ (circles), 0.2 (squares), and 0.3 (diamonds). The inset on the left shows $\sigma/\sqrt{X}$ which exhibits scaling at all temperatures. The inset on the right shows the variation of p_i as a function of the aggregate size i which tends to be uniform at lower temperature.

At lower temperatures clusters of all sizes begin to form with similar weights which results in increasingly large values of σ. For the lattice model, the temperature variations of σ for four different concentrations are shown in figure 12 which exhibits very similar features to those shown in figure 11. The inset shows the corresponding plot for $\sigma/\sqrt{X}$. There is no scaling; however, a crossover of the scaled data in the regime from $T = 0.5$–0.75 is noticeable. This
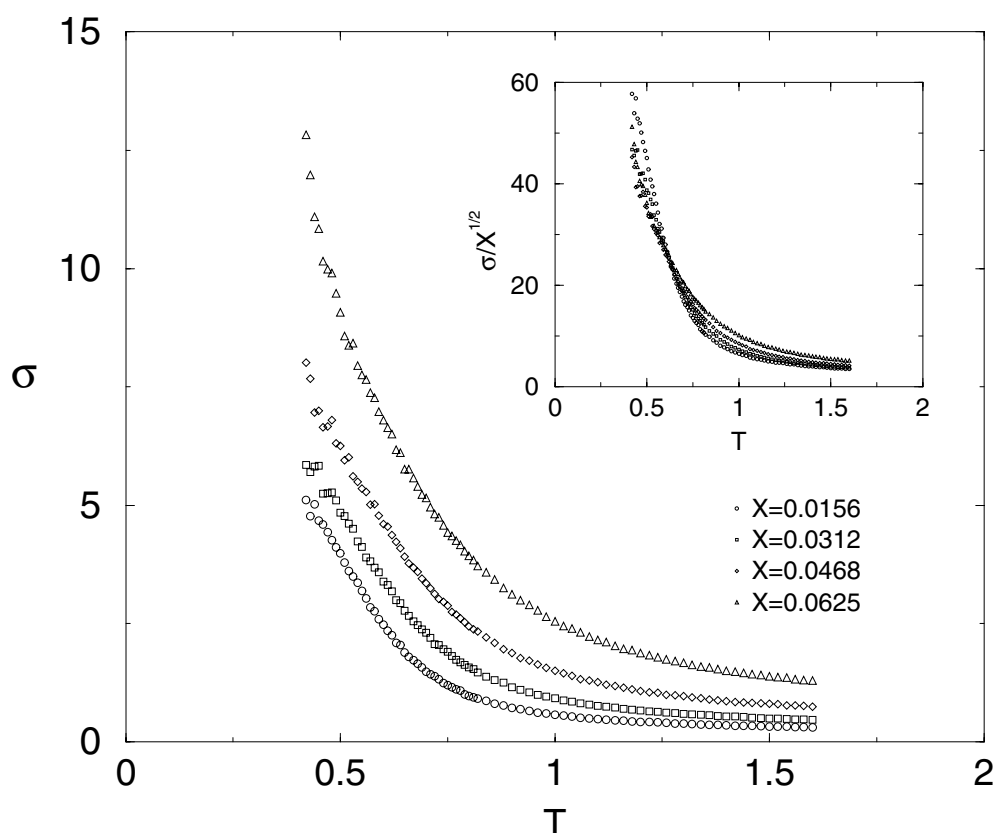
Figure 12. The variation of σ as a function of temperature for $X = 0.0156$ (circles), 0.0312 (squares), 0.0468 (diamonds), and 0.0625 (triangles). The inset shows the corresponding $\sigma/\sqrt{X}$ for the same values of X.

is the same temperature regime for which we observe the Schottky peak. Our results are to be contrasted with the simulation results of σ as a function of temperature given by Care and co-workers [19] which show a peak. In our simulation we did not observe this peak for all the concentrations studied. On the contrary, our results are consistent with the exactly solvable model which we believe to be correct, since the micelles formed in our simulation are quasi-one-dimensional ones.

4. Summary and discussion

In summary, in this paper we have discussed the micellization of amphiphiles in a lattice model and identified the onset of micelle formations with the associated binding energy of any two such amphiphiles. This is the dominant energy scale and most of the essential physics can be understood from the physics of a two-level system. The interaction between the amphiphiles and other effects shifts this scale marginally to a lower temperature. This energy scale is also reflected in the occurrence of a point of inflection and the subsequent flattening of the distribution functions of X_n and X_n/n as functions of cluster size n. This study clarifies the underlying physical picture of the Ruckenstein–Nagarajan criterion of identifying X_{cmc} with the knee of the cluster distribution. Alternatively, this investigation shows that the identification of

the peak in the specific heat for different temperatures can be used as an indicator to characterize X_{cmc}. Naturally this energy scale will be different for different amphiphilic systems. These predictions can be verified experimentally from differential calorimetric measurements and scattering experiments on the same system. For example, the temperature dependence of the specific heat has been investigated experimentally for PEO–PPO–PEO block co-polymers by Alexandris *et al* [43]. However, the systems are different in size and shape to those used in our simulation, but the specific heat exhibits a peak as a function of temperature.

We have also checked that for low concentrations higher-order moments can be obtained from the second moment of the distribution function as predicted by analytic theories. Since the lattice model studied here involves only nearest-neighbour interactions, for low concentrations the interaction term has hardly any effect. Naturally, equation (11) is well satisfied and is a consequence of equation (9) without the interaction term. It will be worthwhile to extend these investigations either to larger concentrations for the neutral amphiphiles, or to ionic micelles, to check how interaction among micelles affects this result. Finally, as we found that in our simulations the observed micelles were mostly elongated, we took a look at the simple theory of one-dimensional micelles and compared the fluctuation of the cluster size with the predictions of this exactly solvable theory. We have found that the quantity σ increases at low temperature and the scaling of $\sigma/\sqrt{X}$ is only approximate. However, the scaled data exhibit a crossover around the same temperature corresponding to the Schottky energy scale of two amphiphiles.

We conclude by mentioning some of the issues that we would like to explore in the future. The argument in favour of an observed peak in the specific heat rests on a discrete energy level structure arising out of the lattice model. In particular, the energy difference $E_{gap} = 4$ comes out of the association of amphiphile chains three units long arranged in linear geometry. It will be interesting to extend the present simulation studies to larger chains which should form spherical micelles. The second issue is that of to what extent these results will be tenable for continuum models. The lattice models can be looked at as a limit of continuum models with short-range interactions. The observed peak in the specific heat is a feature of models with short-range interactions. Therefore we believe that this peak is a generic feature of all models of micellization with a short-range interaction. For the continuum models this peak is likely to be broader. Since previous lattice calculations produce cluster distributions similar to those obtained with a short-range model in the continuum, the observed cluster size fluctuation will still remain valid in the continuum limit. Some of these issues are currently under investigation and will be reported on separately [44].

Acknowledgment

Appendix

Let us define $y = X_1 e^\alpha$. Therefore from equation (17)

$$n_i = \frac{X_i}{i} = y^i e^{-\alpha} \tag{A.1}$$

$$\sum_{i=1}^{\infty} n_i = \sum_{i=1}^{\infty} \frac{X_i}{i} = \sum_{i=1}^{\infty} y^i e^{-\alpha}. \tag{A.2}$$

Let us define

$$S_0 = \sum_{i=1}^{\infty} y^i = \left(\frac{1}{1-y} - 1 \right) = \frac{y}{1-y}. \tag{A.3}$$

It is straightforward to check that the following identity holds for S_0:

$$\sum_{i=1}^{\infty} i^p y^i = \left[y \frac{d}{dy} \right]^p S_0. \tag{A.4}$$

Therefore,

$$\sum_{i=1}^{\infty} n_i = \frac{y}{1-y} e^{-\alpha} \tag{A.5}$$

$$\sum_{i=1}^{\infty} i n_i = \sum_{i=1}^{\infty} X_i = \sum_{i=1}^{\infty} i y^i e^{-\alpha} = y \frac{dS_0}{dy} e^{-\alpha} = \frac{y}{(1-y)^2} e^{-\alpha} \tag{A.6}$$

$$\sum_{i=1}^{\infty} i^2 n_i = \sum_{i=1}^{\infty} i X_i = \sum_{i=1}^{\infty} [i^2 y^i] e^{-\alpha} = y \frac{d}{dy} \left[y \frac{dS_0}{dy} \right] e^{-\alpha} = \frac{y(1+y)}{(1-y)^3} e^{-\alpha}. \tag{A.7}$$

From equations (A.1) and (A.2) it follows that $p_i = (X_1 e^{\alpha})^{i-1} [1 - X_1 e^{\alpha}]$ (equation (19)).

From equation (A.6) we get

$$X = \frac{y}{(1-y)^2} e^{-\alpha} = \frac{X_1}{(1 - X_1 e^{\alpha})^2}. \tag{A.8}$$

Solving the above equation for X_1, one gets equation (20). From equations (13), (A.5), (A.6), and (A.7), it follows that

$$\bar{n} = \frac{1}{1-y} \tag{A.9}$$

$$\left(\sum_{i=1}^{\infty} i^2 n_i \right) \Big/ \left(\sum_{i=1}^{\infty} n_i \right) = \frac{(1+y)}{(1-y)^2}. \tag{A.10}$$

Substituting equations (A.9) and (A.10) in equation (12) we get

$$\sigma = \sqrt{\frac{(1+y)}{(1-y)^2} - \frac{1}{(1-y)^2}} = \sqrt{\frac{y}{(1-y)^2}}. \tag{A.11}$$

From equation (A.8) it then follows that

$$\sigma = \sqrt{X e^{\alpha}} \qquad \text{Q.E.D.} \tag{A.12}$$

References

[1] For reviews, see
Mittal K L and Bothorel P (ed) 1985 *Surfactants in Solution* (New York: Plenum)
Mittal K L and Lindman B (ed) 1984 *Surfactants in Solution* (New York: Plenum)
and other volumes in this series. See also
DeGiorgio V and Corti M (ed) 1985 *Physics of Amphiphiles: Micelles, Vesicles and Microemulsions* (Amsterdam: North-Holland)
[2] Israelachvili J N 1985 *Intermolecular and Surface Forces* (New York: Academic)
[3] Israelachvili J, Mitchell D J and Ninham B W 1976 *J. Chem. Soc., Faraday Trans.* II **72** 1525
[4] Nelson D, Piran T and Wienberg S (ed) 1988 *Statistical Mechanics of Membranes and Surfaces* (Singapore: World Scientific)
[5] Kresge C T, Leonowicz M E, Roth W J, Vertuli J C and Beck J S 1992 *Nature* **359** 710
Huo Q, Margolese D I, Ciesla U, Feng P, Gier T E, Demuth D G, Seger P, Leon R, Petroff P M, Firouzi A, Schuth F and Stucky G D 1994 *Nature* **368** 317
Monnier A, Schuth F, Huo Q, Kumar D, Margolese D, Maxwell R S, Stucky G D, Krishnamurty M, Petroff P, Firouzi A, Janicke M and Chmelka B M 1993 *Science* **261** 1299
[6] Tanev P T and Pinnavaia T J 1995 *Science* **267** 865

Tanev P T and Pinnavaia T J 1996 *Chem. Mater.* **8** 2068
See also
Pinnavaia T J and Thorpe M F (ed) 1995 *Access in Nano-Porous Materials* (New York: Plenum)
Attard G S, Glyde J C and Goltner C J 1995 *Nature* **378** 366

[7] McGrath K M, Dabs D M, Yao N, Aksay I A and Gruner S M 1997 *Science* **277** 552
[8] Bates F S and Fredrickson G H 1999 *Phys. Today* **52** 32
[9] Mukherjee P 1972 *J. Phys. Chem.* **76** 565
[10] Blankschtein D, Thurston G M and Benedek G B 1985 *Phys. Rev. Lett.* **54** 955
Thurston G M, Blankschtein D, Fisch M R and Benedek G B 1986 *J. Chem. Phys.* **84** 4558
Blankschtein D, Thurston G M and Benedek G B 1986 *J. Chem. Phys.* **85** 7268
Puvvada S and Blankschtein D 1990 *J. Chem. Phys.* **92** 3710
[11] Goldstein R E 1986 *J. Chem. Phys.* **84** 3367
[12] Ben-Shaul A, Szleifer I and Gelbart W M 1985 *J. Chem. Phys.* **83** 3597
Szleifer I, Ben-Shaul A and Gelbart W M 1985 *J. Chem. Phys.* **83** 3612
[13] Ruckenstein E and Nagarajan R 1975 *J. Phys. Chem.* **79** 2622
[14] Nagarajan R and Ruckenstein E 1980 *Langmuir* **7** 2934
[15] Ben-Naim A and Stillinger F H 1980 *J. Phys. Chem.* **84** 2872
[16] Stillinger F H and Ben-Naim A 1981 *J. Chem. Phys.* **74** 2510
[17] Egberts E and Berendsen H J C 1988 *J. Chem. Phys.* **89** 3715
[18] Care C M 1987 *J. Phys. C: Solid State Phys.* **20** 689
[19] Care C M 1987 *J. Chem. Soc. Faraday Trans.* **83** 2905
[20] Brindle D and Care C M 1994 *J. Chem. Soc. Faraday Trans.* **88** 2163
[21] Desplat J-C and Care C M 1996 *Mol. Phys.* **87** 441
[22] Larson R G, Scriven L E and Davis H T 1985 *J. Chem. Phys.* **83** 2411
Larson R G 1988 *J. Chem. Phys.* **89** 1642
Larson R G 1989 *J. Chem. Phys.* **91** 2479
Larson R G 1992 *J. Chem. Phys.* **96** 7904
Larson R G 1996 *J. Physique* II **6** 1441
[23] Bernardes A T, Henriques V B and Bisch P M 1994 *J. Chem. Phys.* **101** 645
[24] Bernardes A T 1996 *J. Physique* II **6** 169
[25] Wijmans C J and Linse P 1995 *J. Phys. Chem.* **11** 3748
[26] Rector D R, van Swol F and Henderson J R 1994 *Mol. Phys.* **82** 1009
[27] Smit B, Esselink K, Hilbers P A, van Os N M, Rupert L A M and Szleifer I 1993 *Langmuir* **9** 9
Smit B, Hilbers P A, Esselink K, Rupert L A M and van Os N M 1991 *J. Chem. Phys.* **95** 6361
[28] Palmer B and Liu J 1996 *Langmuir* **12** 746
[29] Palmer B and Liu J 1996 *Langmuir* **12** 6015
[30] Viduna D, Milchev A and Binder K 1998 *Macromol. Theory Simul.* **7** 649
[31] Nelson P H, Rutledge G C and Hatton T A 1997 *J. Chem. Phys.* **107** 10 777
[32] von Gottberg F K, Smith K A and Hatton T A 1997 *J. Chem. Phys.* **106** 9850
[33] Mackie A D, Panagiotopolous A Z and Szleifer I 1997 *Langmuir* **13** 5022
[34] Bhattacharya A, Mahanti S D and Chakrabarti A 1998 *J. Chem. Phys.* **108** 10 281
[35] Bhattacharya A 2000 *J. Chem. Phys.* submitted
[36] Tu K C, Tarek M, Klein M L and Scharf D 1998 *Biophys. J.* **75** 2123
Tu K C, Klein M L and Tobias D J 1998 *Biophys. J.* **75** 2147
[37] Wall F T and Mandel F 1975 *J. Chem. Phys.* **63** 4592
[38] Verdier P H and Stockmayer W H 1962 *J. Chem. Phys.* **36** 227
[39] Phillips J N 1955 *Trans. Faraday Soc.* **51** 561
[40] Pathria R K 1984 *Statistical Mechanics* (Oxford: Pergamon) ch 12
[41] Pathria R K 1984 *Statistical Mechanics* (Oxford: Pergamon) ch 3
[42] Care C M 1997 *Phys. Rev.* E **56** 1181
[43] Alexandris P, Nivaggioli T and Hatton T A 1995 *Langmuir* **11** 1468
[44] Bhattacharya A and Mahanti S D 2000 in preparation